Osteoarthritis and Cartilage 23 (2015) 2206–2213

Osteoarthritis and Cartilage

OARSI OSTEOARTHRITIS RESEARCH SOCIETY INTERNATIONAL

Estimation of articular cartilage properties using multivariate analysis of optical coherence tomography signal

P.H. Puhakka † ‡ *, N.C.R. te Moller §, I.O. Afara †, J.T.A. Mäkelä †, V. Tiitu ‖, R.K. Korhonen †, H. Brommer §, T. Virén ¶, J.S. Jurvelin †, J. Töyräs † ‡

† *Department of Applied Physics, University of Eastern Finland, Kuopio, Finland*
‡ *Department of Clinical Neurophysiology, Kuopio University Hospital, Kuopio, Finland*
§ *Department of Equine Sciences, Utrecht University, Utrecht, Netherlands*
‖ *School of Medicine, Institute of Biomedicine, Anatomy, University of Eastern Finland, Kuopio, Finland*
¶ *Cancer Center, Kuopio University Hospital, Kuopio, Finland*

ARTICLE INFO

Article history:
Received 12 December 2014
Accepted 26 May 2015

Keywords:
Articular cartilage
Optical coherence tomography
Partial least squares regression
Degeneration

SUMMARY

Objective: The aim was to investigate the applicability of multivariate analysis of optical coherence tomography (OCT) information for determining structural integrity, composition and mechanical properties of articular cartilage.

Design: Equine osteochondral samples ($N = 65$) were imaged with OCT, and their total attenuation and backscattering coefficients (μ_t and μ_b) were measured. Subsequently, the Mankin score, optical density (OD) describing the fixed charge density, light absorbance in amide I region (A_{amide}), collagen orientation, permeability, fibril network modulus (E_f) and non-fibrillar matrix modulus (E_m) of the samples were determined. Partial least squares (PLS) regression model was calculated to predict tissue properties from the OCT signals of the samples.

Results: Significant correlations between the measured and predicted mean collagen orientation ($R^2 = 0.75$, $P < 0.0001$), permeability ($R^2 = 0.74$, $P < 0.0001$), mean OD ($R^2 = 0.73$, $P < 0.0001$), Mankin scores ($R^2 = 0.70$, $P < 0.0001$), E_m ($R^2 = 0.50$, $P < 0.0001$), E_f ($R^2 = 0.42$, $P < 0.0001$), and A_{amide} ($R^2 = 0.43$, $P < 0.0001$) were obtained. Significant correlation was also found between μ_b and E_f ($\rho = 0.280$, $P = 0.03$), but not between μ_t and any of the determined properties of articular cartilage ($P > 0.05$).

Conclusion: Multivariate analysis of OCT signal provided good estimates for tissue structure, composition and mechanical properties. This technique may significantly enhance OCT evaluation of articular cartilage integrity, and could be applied, for example, in delineation of degenerated areas around cartilage injuries during arthroscopic repair surgery.

Introduction

Articular cartilage injury can initiate development of osteoarthritis (OA) in both human and animal joints[1,2]. As a consequence to injury, chondrocytes of articular cartilage may die or get damaged, cartilage matrix disruption occurs, and proteoglycan (PG) content decreases, initiating the development of post-traumatic OA[1]. The superficial zone of cartilage is the initial zone in which degenerative changes are typically encountered. In the early stage of cartilage degeneration tissue water content increases and the collagen fibrils are disorganized[3]. These changes further lead to increased permeability and decreased stiffness of articular cartilage.

Several surgical techniques, (e.g., microfracturing and tissue and cell transplantation) are used to repair cartilage injuries and prevent the development of post-traumatic OA[4]. The choice for the optimal repair technique is based on the location and size of the lesion[5], which are usually visually assessed during arthroscopy. However, the detection of early-stage degenerative changes in tissue surrounding the lesion, by means of arthroscopic examination, is difficult[6,7]. To improve treatment planning, it would be beneficial

* Address correspondence and reprint requests to: Puhakka P.H., Department of Applied Physics, University of Eastern Finland, PO Box 1627, 70211 Kuopio, Finland.
E-mail addresses: pia.puhakka@uef.fi (P.H. Puhakka), n.c.r.temoller@uu.nl (N.C.R. te Moller), isaac.afara@uef.fi (I.O. Afara), janne.makela@uef.fi (J.T.A. Mäkelä), virpi.tiitu@uef.fi (V. Tiitu), rami.korhonen@uef.fi (R.K. Korhonen), h.brommer@uu.nl (H. Brommer), tuomas.viren@kuh.fi (T. Virén), jukka.jurvelin@uef.fi (J.S. Jurvelin), juha.toyras@uef.fi (J. Töyräs).

http://dx.doi.org/10.1016/j.joca.2015.05.034
1063-4584/

to have a more accurate, high-resolution arthroscopic technique for diagnosing early-stage degeneration around injuries and to delineate the optimal cartilage region for repair. Identification of early, potentially reversible changes in articular cartilage would also be essential for development of disease-modifying treatment methods[8].

Optical coherence tomography (OCT), an arthroscopically applicable technique, provides adequate resolution (~10–20 μm) for detection and assessment of articular cartilage lesions[9,10]. Morphological features of cartilage surface observed in OCT images agree with the ones found in histological investigation[11]. Furthermore, abnormal organization of collagen fibrils can be detected as a lack of birefringence using polarization sensitive OCT[12]. OCT imaging is based on the measurement of intensity of the light backscattered from different depths of the tissue. The measured intensity depends on light attenuation in the tissue and, at each depth of the tissue, on the amount of light scattering directed to the detector. Microscopic changes in composition and structure of tissues lead to changes in attenuation and scattering properties[13]. Early stage degenerative changes in articular cartilage, like depletion of PGs, could possibly be detected by measuring total attenuation (μ_t) and backscattering (μ_b) coefficients with OCT. To the authors' knowledge, the differences in μ_t or μ_b between normal and degenerated articular cartilage have not been reported. It is known, though, that attenuation is weaker in repair tissue than in native cartilage[14]. Further, the decrease in collagen and chondrocyte contents has been found to decrease light attenuation in agarose scaffolds[15].

Due to its layered nature, articular cartilage exhibits depth-dependent light backscattering and attenuation properties. Therefore, the μ_t and μ_b of the total cartilage thickness layer may not optimally represent this tissue and may not be sensitive enough to detect early stage degeneration. Thus, an alternative analysis approach for OCT data is required. In the present study, the applicability of multivariate partial least squares (PLS) regression to analyse OCT signal and predict cartilage degeneration is studied. This analytical technique has been applied for the analysis of cartilage spectroscopic data[16,17]. The method is used to obtain those features of the multivariate input data (predictor variable) that explain most of the variation in the reference data (response variable) of the sample[18]. We hypothesize that with PLS regression modelling we could obtain a more accurate approximation of articular cartilage properties as compared to measurement of bulk μ_t and μ_b.

Methods

Sample preparation

Osteochondral samples were prepared from metacarpophalangeal joints of healthy, skeletally mature horses ($N = 13$) obtained from a slaughterhouse. Either left or right joint was obtained from eight horses and both from five horses. The horses had a variety of chondral lesions. Osteochondral samples ($N = 65$) were obtained from 1 to 6 anatomical locations within each joint, namely; the tips of the medial and lateral eminences of the first phalanx ($N = 34$), the opposing sites on the medial and lateral condyles ($N = 15$), and the sagittal ridge of the metacarpal bone ($N = 14$). The samples were cut into osteochondral blocks with a minimum surface area of 10×10 mm^2 and the area of interest (e.g., lesion) located in the center.

OCT imaging

The osteochondral samples were imaged using OCT (wavelength 1305 ± 55 nm, axial resolution <20 μm, lateral resolution 25–60 μm; Ilumien PCI Optimization System, St. Jude Medical, St. Paul, MN, USA). During the OCT imaging the samples were immersed in phosphate buffered saline (PBS). The OCT system has a rotating scanning geometry providing cross-sectional images (thickness = 0.1 mm). Each cross-sectional image consists of 504 radial scan lines obtained during one revolution (Fig. 1). The system measures the intensity of the light backscattered at different depths in each scanning direction. Five adjacent cross-sectional images were recorded from each sample. The cartilage surface was automatically detected from the cross-sections, while the cartilage–bone interface was manually determined (by PP). Cartilage thickness in the samples varied between 0.40 mm and 1.39 mm. An average depthwise intensity curve was calculated for an analysis window with a width of 21 scan lines and a height matching the cartilage thickness. Subsequently, average intensity curves of the five cross-sections in each sample were averaged. The first 5% of the curves were excluded during the analyses to avoid specular reflection at the articular surface.

Biomechanical properties

Biomechanical properties of the samples were determined by means of indentation testing. The test was conducted using a custom-made material testing system (resolution for force and deformation, 5 mN and 0.1 μm, respectively)[19]. Cartilage thickness was measured from the OCT image of the sample. The sample was submerged in PBS and a cylindrical plane-ended indenter with a diameter of 530 μm was driven into contact with the sample on the same location where the OCT imaging was conducted. The contact and full recovery of deformation were ensured by indenting the sample 5% of its thickness five times. Then, a stress-relaxation indentation test consisting of two 5% strain steps was performed. Strain rate was 100%/s relative to the thickness of the cartilage. Equilibrium was assumed to be achieved when the slope of relaxation rate was less than 10 Pa/min.

Abaqus (V6.10-1, Dassault Systèmes, Providence, RI, USA) and Matlab (2012a, The MathWorks Inc., Natick, MA, USA) were employed to calculate cartilage biomechanical parameters by fitting an axisymmetric fibril-reinforced poroelastic finite element model to the experimental stress-relaxation data[20–22]. Cartilage was modelled using axisymmetric 4-node continuum pore pressure elements (CAX4P). An elastic fibrillar matrix represented the collagen network and non-fibrillar matrix represented primarily PGs and fluid. The fibrillar matrix was described with organized primary fibrils and randomly organized secondary fibrils[20]. The indenter was modelled as rigid and the cartilage-indenter contact was assumed to be frictionless and impermeable. The cartilage–bone interface was fixed in all directions. The cartilage edge and

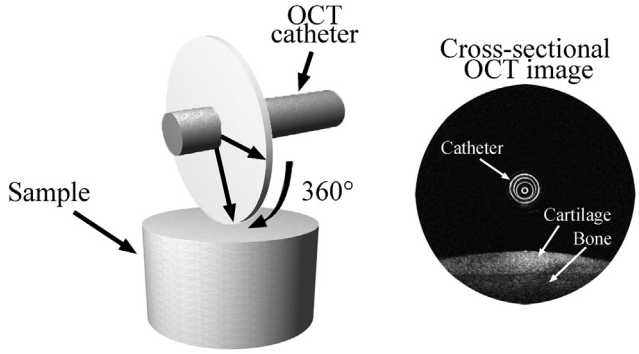

Fig. 1. In the rotational scanning geometry, the OCT system obtains 504 radial scan lines during one 360° revolution to create a cross-sectional image of the sample. The imaging speed is 100 cross-sectional images per second.

the surface not in contact with the indenter were assumed to be fully permeable (zero pore pressure). Mechanical behaviour of the collagen network was expressed with the fibril network modulus (E_f), while non-fibrillar matrix modulus (E_m) and permeability represented the PG/fluid complex. Fluid fraction (80%) and the Poisson's ratio of the non-fibrillar matrix (0.42) were fixed in the model[22,23], whereas E_f, E_m and permeability were obtained by minimizing the mean square error between the reaction forces in the experiment and finite element model. Since the first step was considered as a pre-strain, the optimization was performed only for the second step.

Histology

After indentation testing, the samples were stored in a freezer (−20°C). For histological and spectroscopical analyses, the osteochondral samples were thawed, immersed in formalin for at least 48 h, and then decalcified in ethylenediaminetetraacetic acid. After further processing, three Safranin-O stained sections (thickness = 3 μm) for histological evaluation and three unstained sections (thickness = 5 μm) for spectroscopical analyses were prepared from the measurement site of each sample.

The stained sections were examined with a light microscope (Axio Imager M2, Carl Zeiss MicroImaging, Jena, Germany). Histological integrity of the samples were evaluated from their images by assigning Mankin scores[24]. The images of the three sections from each sample were blindly coded and scored by three investigators (NtM, JT, and VT). The final score was calculated as an average of the scores rounded to the nearest integer. Based on Mankin scores, the samples were further divided into two groups by the severity of the degeneration; from no to mild degeneration (Mankin scores 0–6) and from moderate to severe degeneration (Mankin scores 7–14)[25].

Depthwise PG distribution (fixed charge density) was estimated from optical density (OD) of the grayscale images of Safranin-O stained sections captured with a light microscope and a CCD camera (SenSys, Photometrics Inc., USA)[26]. The final OD distribution was obtained as the average OD distribution of the three sections.

Fourier transform infrared spectroscopy and polarized light microscopy

Light absorbance in amide I region (A_{amide}; 1594–1720 cm^{-1}), representative of the collagen content, was assessed as a mean absorbance distribution in the three unstained sections using Fourier transform infrared spectroscopy (FTIR; Spotlight 300 FTIRI, Perkin Elmer, Shelton, CT, USA) analysis[27]. Collagen orientation with respect to cartilage surface direction was determined by means of polarized light microscopy (Ortholux II POL; Leitz Wetzlar, Wetzlar, Germany) based on Stokes parameters[28,29].

OCT analysis: total attenuation and backscattering coefficient

μ_t and μ_b were determined by fitting the mean depthwise OCT intensity curve, $I(d)$, into the following equation[30]:

$$I(d) \propto \sqrt{\mu_b}\ \frac{1}{\sqrt{\left(\frac{d-d_0}{z_0}\right)^2 + 1}} \exp(-\mu_t d), \tag{1}$$

where d is the probing depth in cartilage, d_0 beam focus position and z_0 the apparent Rayleigh length. Prior to fitting, the OCT system was calibrated using suspension series of water and polystyrene spheres (diameter = 5 μm; Phosphores Inc., Hopkinton, MA, USA).[15]

OCT analysis: PLS regression multivariate analysis

PLS regression models were developed to estimate cartilage properties based on depth-dependent OCT signal. Multivariate PLS regression is an analytical technique for relating potentially correlated and noisy predictor variables to one or several response variables by finding a linear regression between them in a new space[18]. Briefly, developed and validated PLS regression models that optimize the relationship between the predictor and response variables are used to predict the response variables of new samples from predictor variables. In the present study, the OCT intensity curves were smoothed using a fourth degree Savitzky-Golay filter and the second derivatives of the smoothed intensity curves were used as predictor variables in the PLS analyses. Mankin score, severity of degeneration, E_f, E_m, permeability and averages of OD, A_{amide}, and collagen orientation within the whole cartilage layer, the superficial zone (10% of cartilage thickness), the middle zone (15%) and the deep zone (75%) of the cartilage served as response variables.

Leave-one-out cross-validation was computed in order to determine the optimal number of PLS components of the models[31]. Too few components may result in under-fitting, while too many may yield over-fitted models. In leave-one-out cross-validation each sample is left out one by one and the other samples are used to predict the response property of the sample left out. The criteria for optimal model selection were based on the model with the highest coefficient of determination (R^2) and the lowest root mean square error of cross-validation (RMSECV). Model performance was evaluated by predicting the cartilage properties of the samples from their OCT signals using the created model[32,33]. The root mean square error of prediction (RMSEP) was calculated from the deviation between the predicted and true response parameter values ($\hat{y}$ and y, respectively):

$$RMSEP = \sqrt{\frac{\sum_{i=1}^{n} (\hat{y}_i - y_i)^2}{n}}, \tag{2}$$

where n is the number of the samples. For data pre-processing and multivariate analyses, custom-written software utilizing the SIMPLS algorithm in Matlab (2014a; MathWorks, Inc., Natic, MA, USA) was used.

Statistical analyses

Relationships of μ_t and μ_b with other determined properties of articular cartilage were evaluated by calculating Spearman's rank correlation coefficients (IBM SPSS Statistics 19, SPSS Inc., Chicago, USA). A monotonic relationship of μ_t and μ_b with the cartilage properties was assumed.

Results

Mean (standard deviation) for μ_t and μ_b of the samples were 2.2 mm^{-1} (1.1 mm^{-1}) and 13.4 mm^{-1} (7.9 mm^{-1}), respectively. Mean and standard deviation of Mankin score, permeability, E_m, E_f, OD, A_{amide} and collagen orientation are presented in Table I. A significant linear correlation was found between μ_b and E_f, but not between μ_b and the Mankin score, k, E_m, OD, A_{amide} or collagen orientation (Table II). The μ_t values did not correlate significantly with any of the cartilage properties (Table II).

In the PLS analyses, three to seven PLS components were found to be optimal in the regression models created between OCT intensity curve and the different properties of articular cartilage. Correlations between the measured properties of articular cartilage and those predicted using PLS models were high for Mankin score

Table I
Mean and standard deviation for various properties of articular cartilage (response variables) and the PLS regression statistics for prediction of the variables based on depthwise OCT intensity curves

Response variable	Zone	Mean of response variable	Std of response variable	Number of components	RMSEP	R^2
Mankin score	All	3.5	2.6	5	1.4	0.70
Permeability ($\times 10^{-15}$ $m^4N^{-1}s^{-1}$)	All	5.5	8.7	5	4.4	0.74
E_m (MPa)	All	0.25	0.24	3	0.17	0.50
E_f (MPa)	All	1.74	1.18	3	0.89	0.42
OD (arb. unit)	All	1.42	0.37	5	0.16	0.73
	Superficial	0.67	0.40	6	0.18	0.79
	Middle	1.20	0.55	6	0.25	0.79
	Deep	1.57	0.35	6	0.16	0.80
A_{amide} (arb. unit)	All	42.0	4.9	4	3.7	0.43
	Superficial	23.6	4.6	5	2.7	0.64
	Middle	30.7	5.0	5	3.2	0.57
	Deep	46.7	5.3	5	8.8	0.56
Collagen orientation (deg)	All	66.2	14.4	7	7.1	0.75
	Superficial	35.9	17.0	4	11.3	0.55
	Middle	58.7	16.1	4	10.6	0.56
	Deep	71.7	16.8	4	11.8	0.50

Std = standard deviation, RMSEP = root mean square error in prediction, R^2 = coefficient of determination, E_m = non-fibrillar matrix modulus, E_f = fibril network modulus, OD = optical density, A_{amide} = FTIR absorbance in amide I region.

Table II
Linear correlations between the measured compositional, structural and biomechanical properties of articular cartilage and its light attenuation and backscattering coefficients (μ_t and μ_b, respectively) indicated by Spearman's rank correlation coefficients (*rho*) and the corresponding *P*-values

	Mankin score	Permeability ($\times 10^{-15}$ $m^4N^{-1}s^{-1}$)	E_m (MPa)	E_f (MPa)	OD (arb. unit)	A_{amide} (arb. unit)	Collagen orientation (deg)
μ_t (mm^{-1})	*rho* = 0.019	*rho* = −0.043	*rho* = 0.107	*rho* = 0.093	*rho* = −0.021	*rho* = 0.071	*rho* = 0.129
	P = 0.88	*P* = 0.74	*P* = 0.41	*P* = 0.47	*P* = 0.87	*P* = 0.58	*P* = 0.31
μ_b (mm^{-1})	*rho* = −0.026	*rho* = −0.128	*rho* = 0.166	*rho* = 0.280	*rho* = 0.086	*rho* = 0.241	*rho* = 0.138
	P = 0.84	*P* = 0.33	*P* = 0.20	*P* = 0.03	*P* = 0.50	*P* = 0.06	*P* = 0.28

E_m = non-fibrillar matrix modulus, E_f = fibril network modulus, OD = optical density, A_{amide} = FTIR absorbance in amide I region, μ_t = total attenuation coefficient, μ_b = backscattering coefficient.

(R^2 = 0.70, RMSEP = 1.4), permeability (R^2 = 0.74, RMSEP = 4.4×10^{-15} $m^4N^{-1}s^{-1}$), bulk OD ($R^2 = 0.73$, RMSEP = 0.16 arb. unit) and OD in different zones of the articular cartilage ($R^2 \geq 0.79$, RMSEP ≤ 0.25 arb. unit) (Table I). Correlation between the predicted and measured bulk collagen orientation was good ($R^2 \geq 0.75$, RMSEP = 7.1°), but even if the number of PLS coefficients was further reduced, the error in cross-validation remained high compared to the standard deviation of the measured orientation values. Moderate and significant correlations ($R^2 < 0.70$, $P < 0.0001$) were found between the measured and predicted E_m, E_f and A_{amide} of the articular cartilage samples (Table I). The relations between the predicted and measured bulk properties of the samples are presented in Fig. 2. Bland–Altman plots show the agreement between the measured and predicted properties of the samples (Fig. 3). Nine of all samples were initially grouped into the category of moderate to severe degeneration based on their Mankin scores. Six of those samples were similarly diagnosed when the severity of degeneration was predicted using the PLS model.

Discussion

The diagnostic value of conventional arthroscopic evaluation is limited when assessing early stage cartilage degeneration due to subjectivity[6]. The application of OCT under arthroscopic guidance provides more detailed images of the cartilage lesions and enhances the reproducibility of cartilage lesion scoring[34]. In addition, OCT could also be used to investigate microstructural tissue changes. The present study demonstrates the diagnostic potential of OCT via multivariate analysis, in assessment of degenerative changes in the composition, structure, and mechanical properties of articular cartilage.

Based on the results, the bulk attenuation and backscattering parameters, determined from OCT signal, were not sensitive enough to detect small compositional changes in articular cartilage. Both collagen and chondrocytes scatter light and affect the OCT signal[15]. However, possible changes in their content during degeneration were not revealed by measuring μ_t or μ_b. The sensitivity of the bulk attenuation coefficient for early osteoarthritic changes in articular cartilage was also questioned by Nebelung *et al.*[35] This supports the choice of multivariate analysis of the OCT signal for detailed diagnostic purposes.

The PLS models constructed based on the measured OCT signals provided high correlation especially between the measured and the predicted values of Mankin score, permeability, OD, and bulk collagen orientation. All the samples having no or mild degeneration were correctly classified by predicting their Mankin scores, whereas three out of nine samples were misclassified to have no to mild degeneration as opposed to moderate to severe degeneration. Permeability does not have direct effect on the optical properties of articular cartilage, but it is a good measure of many simultaneous changes in composition and structure of the tissue during degeneration. The permeability of articular cartilage relates to the PG content of the tissue[36]. Therefore, the contribution of PGs to OCT signal may be the reason for the correlation between the measured and predicted permeability. In the present study, OD was used as the measure of PG content. Earlier, PGs have not been shown to affect the birefringence[37] or surface reflection[38] when measured by OCT. However, the present high correlation between measured OD and OD predicted by the PLS model might indicate a contribution of PGs to OCT light backscattering. The influence of PGs on OCT signal is of great interest as PG depletion, in addition to disorganization of collagen matrix, is one of the first signs of cartilage degeneration[39,40].

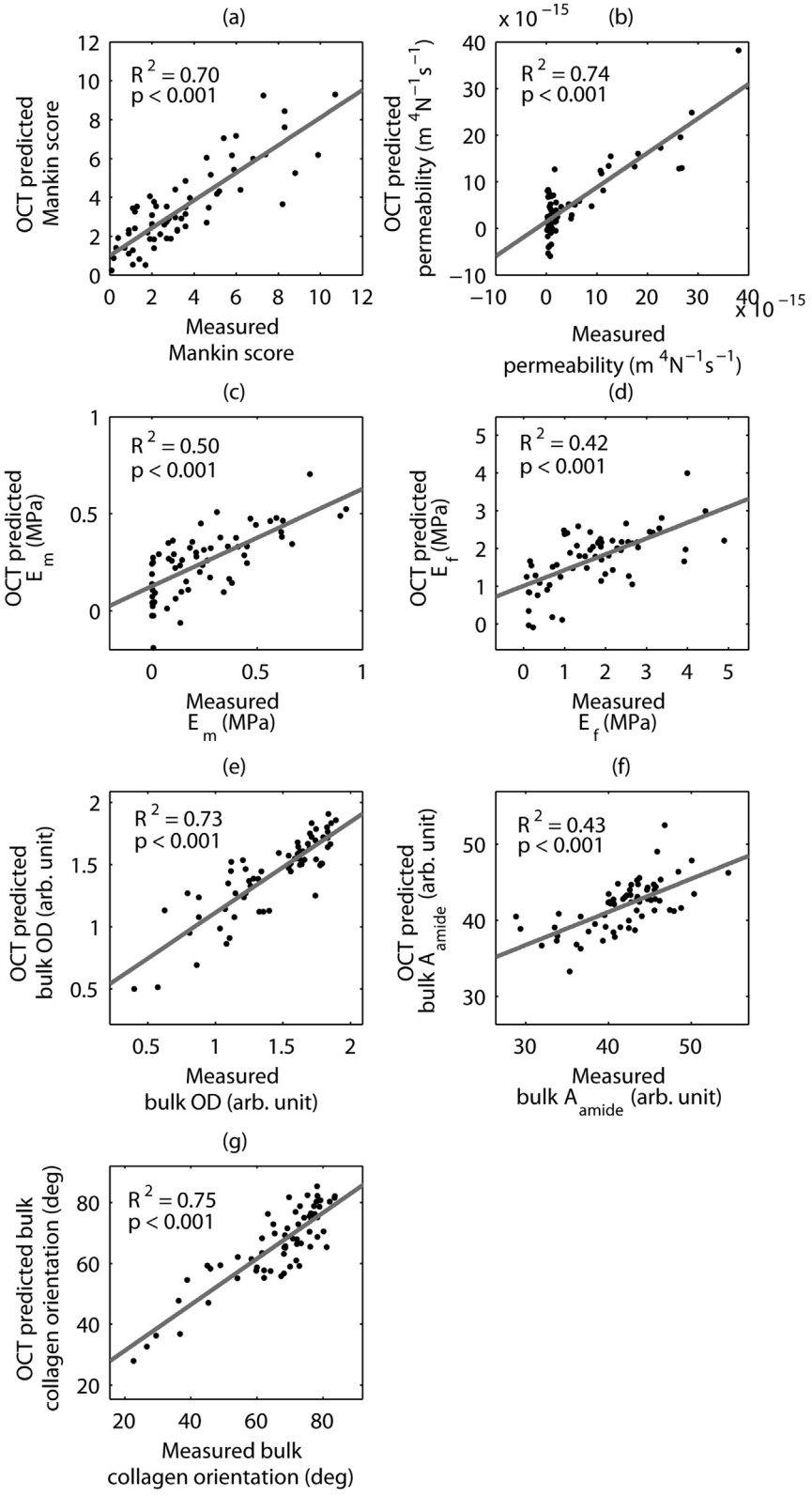

Fig. 2. The measured bulk properties of articular cartilage and those predicted from OCT signal using PLS regression models. (a) Mankin score, (b) permeability, (c) non-fibrillar matrix modulus (E_m) (d) fibril network modulus (E_f) (e) bulk OD (f) bulk FTIR absorbance in amide I region (A_{amide}) and (g) bulk collagen orientation.

It is worth noting that the OCT system used in this study was not designed for measurement of birefringence. Hence, the significant relation between the OCT signal and collagen orientation may result, in part, from varying scattering properties of fibrils oriented at different angles as well as from other compositional and structural properties that change simultaneously with disorganization of the collagen network. However, the measurement of birefringence would be a valuable addition for identification of early

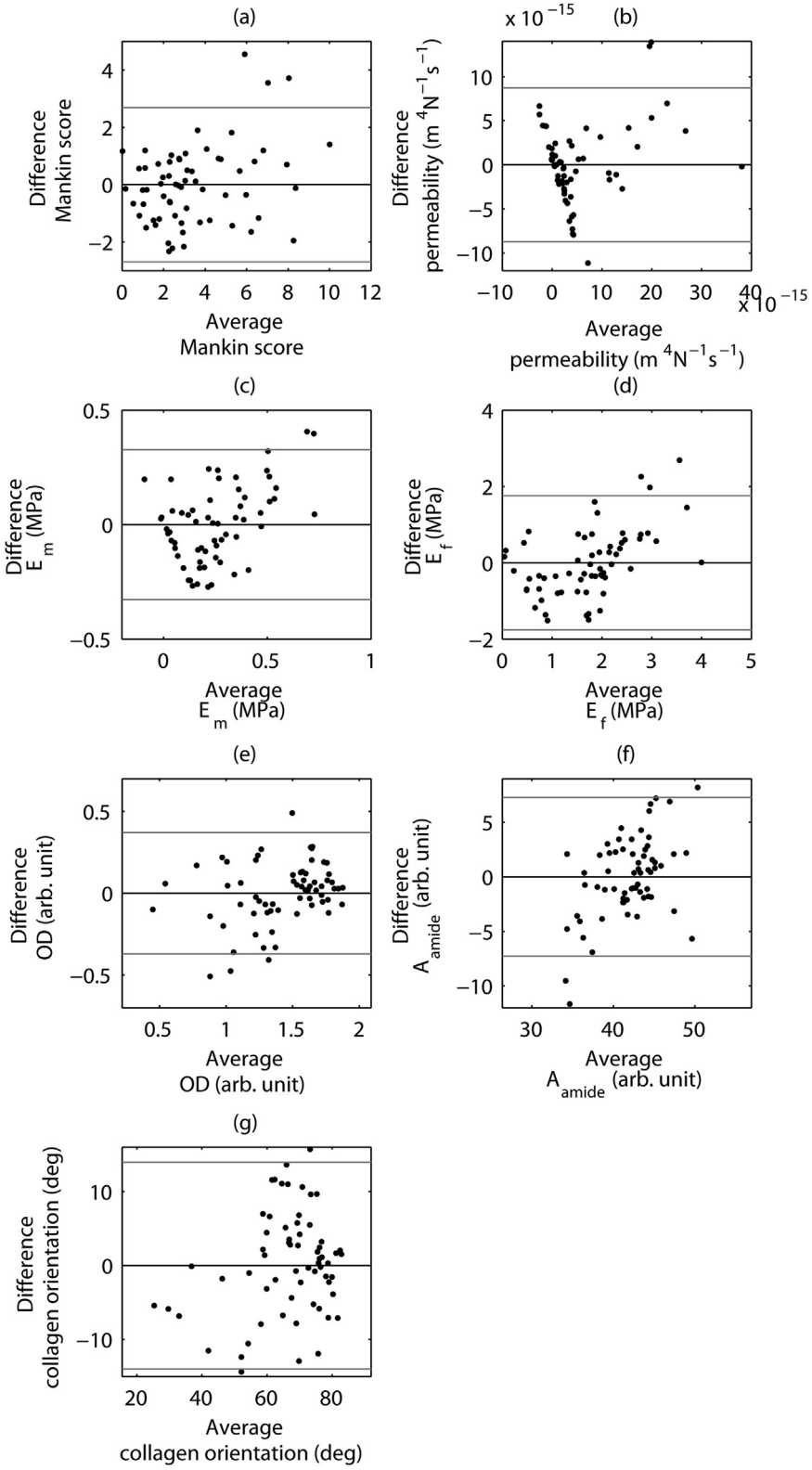

Fig. 3. Bland–Altman plots representing the average and difference of measured and predicted articular cartilage (a) Mankin score, (b) permeability, (c) non-fibrillar matrix modulus (E_m) (d) fibril network modulus (E_f) (e) bulk OD (f) bulk FTIR absorbance in amide I region (A_{amide}) and (g) bulk collagen orientation.

cartilage degeneration[7]. Additionally, the use of an ultra-high resolution OCT system could improve the detection of the depthwise changes in the amount of small scattering components. The use of higher resolution would also increase the number of predictor variables in the model, and could possibly improve the accuracy of the PLS predictive model.

The relationship between the measured and predicted FTIR absorbance in amide I region (i.e., collagen content) was not strong

($R^2 = 0.43$). Mechanical properties of articular cartilage are related to collagen matrix properties[20,41]. Therefore, the relation of OCT signal to fibril network modulus may reflect its relation to collagen content and organization. In early stage of degeneration, the collagen content abides although the fibril organization changes[3]. Therefore, the assessment of collagen content may be of minor importance when differentiating healthy cartilage from areas with signs of the earliest stage of degeneration.

Due to the limited light penetration, OCT imaging cannot be conducted non-invasively, but is a useful tool in arthroscopies[9,10]. Presently, with thin equine cartilage, the prediction ability of the PLS models was similar for each of the three cartilage zones. In OCT analysis, the structural and compositional properties in the superficial zone of articular cartilage may have the highest diagnostic value. The limited penetration depth (1–2 mm[42]) of the light might hinder the ability to analyse middle and deep zones of thick human articular cartilage. By choosing adequate central wavelength for the OCT light, the light penetration could be marginally improved[43]. However, the optimal choice of wavelength is a sensitive balance between increase in water absorption and decrease of scattering[44]. Further studies with human cartilage are needed to investigate if the evaluation of cartilage only to depth of 1–2 mm is sufficient for the diagnostics.

Following our hypothesis, multivariate analyses of depthwise optical intensity signal from OCT images of articular cartilage has potential to provide information on tissue compositional, structural and mechanical properties that are otherwise non-accessible from bulk attenuation and backscattering properties. However, Bland–Altman analysis showed a higher accuracy of the models for cartilage with no or mild degenerative changes. This arises from the under-representation of cartilage with advanced degeneration in the sample set. The errors obtained in the present study should be reduced for research purposes, but could be satisfactory for diagnostics as small errors may not affect clinical decisions. Nevertheless, the approach needs to be further validated and optimized before it can be applied clinically. For example, test set validation, which uses a set of test samples independent of the training set, could be used to further validate the performance of the multivariate models developed in this study. Further, doubling the amount of samples in training of the PLS model may improve the accuracy of the assessment and would enable use of the test set validation[18]. Adequate diagnostic accuracy and good intra- and inter-observer agreements in both model creation and prediction of cartilage properties are required, and they need to be thoroughly evaluated.

Quantitative OCT analysis could improve the evaluation of articular cartilage integrity. After careful calibration and validation of the PLS model, the use of the model for prediction of cartilage properties could be fast and feasible in clinical use. The present technique might be used in arthroscopic surgery in order to delineate degenerated areas around articular cartilage lesions and to aid the selection of the optimal treatment method.

Author contributions

Conception and design of the study: All authors.
Acquisition of data: Puhakka, te Moller.
Analysis and interpretation of data: All authors.
Critical revision and approval of the final submitted version of the article: All authors.
Responsibility for the integrity of the work as a whole: Puhakka, Töyräs.

Role of the funding sources

Funding was received from Jenny and Antti Wihuri Foundation, Academy of Finland (132367, 267551), University of Eastern Finland (Spearhead 931053) and Kuopio University Hospital (5041723, 5041738). The funding sources did not play any role in the study design, data collection or analysis, writing the manuscript, or decision to submit the manuscript for publication.

Competing interest statement

None of the authors have conflict of interest.

Acknowledgements

Eija Rahunen and Simo Ojanen are acknowledged for technical assistance.

References

1. Buckwalter JA, Brown TD. Joint injury, repair, and remodeling: roles in post-traumatic osteoarthritis. Clin Orthop Relat Res 2004:7–16.
2. Caron JP. Osteoarthritis. In: Ross MWDSJ, Ed. Diagnosis and Management of Lameness in the Horses. Missouri: Elsevier Science; 2011:655–67.
3. Buckwalter JA, Mankin HJ. Articular cartilage. Part II: degeneration and osteoarthrosis, repair, regeneration, and transplantation. J Bone Joint Surg Am 1997;79:612–32.
4. Hunziker EB. Articular cartilage repair: basic science and clinical progress. A review of the current status and prospects. Osteoarthritis Cartilage 2002;10:432–63.
5. Gomoll AH, Filardo G, de Girolamo L, Esprequeira-Mendes J, Marcacci M, Rodkey WG, *et al*. Surgical treatment for early osteoarthritis. Part I: cartilage repair procedures. Knee Surg Sport Tr A 2012;20:450–66.
6. Brismar BH, Wredmark T, Movin T, Leandersson J, Svensson O. Observer reliability in the arthroscopic classification of osteoarthritis of the knee. J Bone Joint Surg Br 2002;84:42–7.
7. Chu CR, Williams A, Tolliver D, Kwoh CK, Bruno 3rd S, Irrgang JJ. Clinical optical coherence tomography of early articular cartilage degeneration in patients with degenerative meniscal tears. Arthritis Rheum 2010;62:1412–20.
8. Chu CR, Williams AA, Coyle CH, Bowers ME. Early diagnosis to enable early treatment of pre-osteoarthritis. Arthritis Res Ther 2012;14:212.
9. Pan YT, Li ZG, Xie TQ, Chu CR. Hand-held arthroscopic optical coherence tomography for *in vivo* high-resolution imaging of articular cartilage. J Biomed Opt 2003;8:648–54.
10. te Moller NC, Brommer H, Liukkonen J, Virén T, Timonen M, Puhakka PH, *et al*. Arthroscopic optical coherence tomography provides detailed information on articular cartilage lesions in horses. Vet J 2013;197:589–95.
11. Chu CR, Lin D, Geisler JL, Chu CT, Fu FH, Pan YT. Arthroscopic microscopy of articular cartilage using optical coherence tomography. Am J Sport Med 2004;32:699–709.
12. Drexler W, Stamper D, Jesser C, Li X, Pitris C, Saunders K, *et al*. Correlation of collagen organization with polarization sensitive imaging of *in vitro* cartilage: implications for osteoarthritis. J Rheumatol 2001;28:1311–8.
13. Xu CY, Schmitt JM, Carlier SG, Virmani R. Characterization of atherosclerosis plaques by measuring both backscattering and attenuation coefficients in optical coherence tomography. J Biomed Opt 2008;13:034003.
14. Cernohorsky P, Kok AC, Bruin DM, Brandt MJ, Faber DJ, Tuijthof GJ, *et al*. Comparison of optical coherence tomography

and histopathology in quantitative assessment of goat talus articular cartilage. Acta Orthop 2015;86:257–63.
15. Puhakka PH, Ylärinne JH, Lammi MJ, Saarakkala S, Tiitu V, Kröger H, *et al*. Dependence of light attenuation and back-scattering on collagen concentration and chondrocyte density in agarose scaffolds. Phys Med Bio 2014;59:6537–48.
16. Li GY, Thomson M, Dicarlo E, Yang X, Nestor B, Bostrom MPG, *et al*. A chemometric analysis for evaluation of early-stage cartilage degradation by infrared fiber-optic probe spectroscopy. Appl Spectrosc 2005;59:1527–33.
17. Afara I, Prasadam I, Crawford R, Xiao Y, Oloyede A. Non-destructive evaluation of articular cartilage defects using near-infrared (NIR) spectroscopy in osteoarthritic rat models and its direct relation to Mankin score. Osteoarthritis Cartilage 2012;20:1367–73.
18. Wold S, Sjöström M, Eriksson L. PLS-regression: a basic tool of chemometrics. Chemom Intell Lab Syst 2001;58:109–30.
19. Töyräs J, Rieppo J, Nieminen MT, Helminen HJ, Jurvelin JS. Characterization of enzymatically induced degradation of articular cartilage using high frequency ultrasound. Phys Med Biol 1999;44:2723–33.
20. Julkunen P, Kiviranta P, Wilson W, Jurvelin JS, Korhonen RK. Characterization of articular cartilage by combining microscopic analysis with a fibril-reinforced finite-element model. J Biomech 2007;40:1862–70.
21. Mäkelä JTA, Huttu MRJ, Korhonen RK. Structure-function relationships in osteoarthritic human hip joint articular cartilage. Osteoarthritis Cartilage 2012;20:1268–77.
22. Korhonen RK, Laasanen MS, Töyräs J, Lappalainen R, Helminen HJ, Jurvelin JS. Fibril reinforced poroelastic model predicts specifically mechanical behavior of normal, proteoglycan depleted and collagen degraded articular cartilage. J Biomech 2003;36:1373–9.
23. Li LP, Soulhat J, Buschmann MD, Shirazi-Adl A. Nonlinear analysis of cartilage in unconfined ramp compression using a fibril reinforced poroelastic model. Clin Biomech 1999;14:673–82.
24. Mankin HJ, Dorfman H, Lippiello L, Zarins A. Biochemical and metabolic abnormalities in articular cartilage from osteo-arthritic human hips. II. Correlation of morphology with biochemical and metabolic data. J Bone Joint Surg Am 1971;53:523–37.
25. Ehrlich MG, Houle PA, Vigliani G, Mankin HJ. Correlation between articular-cartilage collagenase activity and osteoarthritis. Arthr Rheum 1978;21:761–6.
26. Király K, Lapvetelainen T, Arokoski J, Törrönen K, Modis L, Kiviranta I, *et al*. Application of selected cationic dyes for the semiquantitative estimation of glycosaminoglycans in histological sections of articular cartilage by microspectrophotometry. Histochem J 1996;28:577–90.
27. Boskey A, Pleshko Camacho N. FT-IR imaging of native and tissue-engineered bone and cartilage. Biomaterials 2007;28:2465–78.
28. Massoumian F, Juskaitis R, Neil MAA, Wilson T. Quantitative polarized light microscopy. J Microsc-Oxford 2003;209:13–22.
29. Rieppo J, Hallikainen J, Jurvelin JS, Kiviranta I, Helminen HJ, Hyttinen MM. Practical considerations in the use of polarized light microscopy in the analysis of the collagen network in articular cartilage. Microsc Res Tech 2008;71:279–87.
30. Faber DJ, van der Meer FJ, Aalders MCG, van Leeuwen TG. Quantitative measurement of attenuation coefficients of weakly scattering media using optical coherence tomography. Opt Express 2004;12:4353–65.
31. Lorber A, Kowalski BR. Alternatives to cross-validatory estimation of the number of factors in multivariate calibration. Appl Spectrosc 1990;44:1464–70.
32. Wang LQ, Chapman J, Palmer RA, Alter TM, Hooper BA, van Ramm O, *et al*. Classification of atherosclerotic rabbit aorta samples with an infrared attenuated total reflection catheter and multivariate data analysis. Appl Spectrosc 2006;60:1121–6.
33. Afara IO, Prasadam I, Moody H, Crawford R, Xiao Y, Oloyede A. Near infrared spectroscopy for rapid determination of Mankin score components: a potential tool for quantitative characterization of articular cartilage at surgery. Arthroscopy 2014;30:1146–55.
34. Niemelä T, Virén T, Liukkonen J, Argüelles D, te Moller NC, Puhakka PH, *et al*. Application of optical coherence tomography enhances reproducibility of arthroscopic evaluation of equine joints. Acta Vet Scand 2014;56:3.
35. Nebelung S, Marx U, Brill N, Arbab D, Quack V, Jahr H, *et al*. Morphometric grading of osteoarthritis by optical coherence tomography - an ex vivo study. J Orthop Res 2014;32:1381–8.
36. Maroudas A. Physicochemical properties of articular cartilage. In: Freeman MAR, Ed. Adult Articular Cartilage. Kent: Pitman Medical Publishing; 1979:215–90.
37. Xie T, Guo S, Zhang J, Chen Z, Peavy GM. Determination of characteristics of degenerative joint disease using optical coherence tomography and polarization sensitive optical coherence tomography. Lasers Surg Med 2006;38:852–65.
38. Saarakkala S, Wang SZ, Huang YP, Zheng YP. Quantification of the optical surface reflection and surface roughness of articular cartilage using optical coherence tomography. Phys Med Bio 2009;54:6837–52.
39. Martel-Pelletier J, Boileau C, Pelletier JP, Roughley PJ. Cartilage in normal and osteoarthritis conditions. Best Pract Res Cl Rh 2008;22:351–84.
40. Mäkelä JTA, Rezaeian ZS, Mikkonen S, Madden R, Han SK, Jurvelin JS, *et al*. Site-dependent changes in structure and function of lapine articular cartilage 4 weeks after anterior cruciate ligament transection. Osteoarthritis Cartilage 2014;22:869–78.
41. Mow VC, Ratcliffe A, Poole AR. Cartilage and diarthrodial joints as paradigms for hierarchical materials and structures. Biomaterials 1992;13:67–97.
42. Drexler W. Ultrahigh-resolution optical coherence tomography. J Biomed Opt 2004;9:47–74.
43. Sharma U, Chang EW, Yun SH. Long-wavelength optical coherence tomography at 1.7 mu m for enhanced imaging depth. Opt Express 2008;16:19712–23.
44. Bouma BE, Nelson LE, Tearney GJ, Jones DJ, Brezinski ME, Fujimoto JG. Optical coherence tomographic imaging of human tissue at 1.55 mu m and 1.81 mu m using Er- and Tm-doped fiber sources. J Biomed Opt 1998;3:76–9.